

黑钨矿有效沉淀机制: CO_2 逃逸

刘向冲^{1,2}, 张德会³

- (1. 中国地质科学院地质力学研究所, 北京 100081;
2. 中国地质科学院地质力学研究所动力成岩成矿实验室, 北京 100081;
3. 中国地质大学(北京) 地球科学与资源学院, 北京 100083)

摘要: 黑钨矿是石英脉钨矿床的主要矿石矿物, 其沉淀机制一直存在争议。 CO_2 逃逸能否造成黑钨矿有效沉淀尚缺乏定量模型的评价。文章建立了 W-Fe-Cl-Na-O-C-H 体系的反应平衡模型, 涉及 22 种组分和 16 个化学反应; 相关热力学参数来自 SUPCRT 数据库。模型计算结果表明, pH 与流体压力呈负相关关系, 而钨溶解度与流体压力呈正相关关系; 当成矿流体压力从静岩压力降至静水压力水平, 钨溶解度降幅可达到 27%~47%, 降幅与温度和深度成正比。因而, 降压造成的 CO_2 逃逸是黑钨矿沉淀的有效机制之一。

关键词: 黑钨矿; 沉淀机制; CO_2 逃逸; 平衡反应模型

中图分类号: P618. 67 文献标识码: A

THE EFFICIENT MECHANISMS FOR PRECIPITATING WOLFRAMITE: CO_2 ESCAPING

LIU Xiangchong^{1,2}, ZHANG Dehui³

- (1. Institute of Geomechanics, Chinese Academy of Geological Sciences, Beijing 100081, China;
2. The Laboratory of Dynamic Digenesis and Metallogenesis, Institute of Geomechanics, CAGS, Beijing 100081, China;
3. School of Earth Sciences and Resources, China University of Geosciences (Beijing), Beijing 100083, China)

Abstract: Wolframite is the main ore mineral of vein-type tungsten deposits. How wolframite precipitates from hydrothermal fluids is highly disputed in the literature. Whether CO_2 escaping causes significant precipitation of wolframite has not been quantitatively examined. A reaction equilibrium model for the system of W-Fe-Na-Cl-H-C-O was established in this contribution. The model contains 22 species and 16 reactions, the thermodynamic data of which are from the database SUPCRT. The modeling results indicate that pH is negatively correlated to fluid pressure and tungsten solubility is positively correlated to fluid pressure. A decrease in fluid pressure from lithostatic to hydrostatic level could cause a drop of tungsten solubility by 27%~47%, and the decrease degree has a positive correlation to temperature and depth. Therefore, CO_2 escaping accompanying a drop of fluid pressure is one of the mechanisms precipitating wolframite efficiently.

Key words: wolframite; precipitation mechanism; CO_2 escaping; equilibrium reaction modeling

基金项目: 中国地质科学院基本科研业务费 (JYYWF20180602, DZLXJK201603); 国家自然科学基金 (41602088, 41402295)

作者简介: 刘向冲 (1987-), 男, 副研究员, 从事成矿动力学和数学地质等研究。E-mail: xcliu@cags.ac.cn

收稿日期: 2018-10-11; 修回日期: 2018-12-18; 责任编辑: 吴芳

引用格式: 刘向冲, 张德会. 黑钨矿有效沉淀机制: CO_2 逃逸 [J]. 地质力学学报, 2019, 25 (1): 19~26 DOI: 10.12090/j.issn.1006-6616.2019.25.01.003

LIU Xiangchong, ZHANG Dehui. The efficient mechanisms for precipitating wolframite: CO_2 escaping [J]. Journal of Geomechanics, 2019, 25 (1): 19~26 DOI: 10.12090/j.issn.1006-6616.2019.25.01.003

钨矿是一种岩浆热液型矿床，主要的矿石矿物有白钨矿和黑钨矿^[1~2]。其中，黑钨矿主要赋存在石英脉型黑钨矿床，其沉淀机制存在争议^[3~5]。柳志青^[3]根据黑钨矿在石英脉中的分布规律，提出矿物微粒浓差运离分带的假说，定性地解释黑钨矿集合体（钨砂包）的生长机制。有学者提出钨成矿流体为富硅的岩浆热液过渡性流体，而非简单的热水溶液^[4,6~7]。一些学者利用流体包裹体、稳定同位素、高温高压实验和计算模拟等方法提出黑钨矿可能有四种沉淀方式：①简单降温^[8~9]；②岩浆水与大气降水混合^[10]；③水岩反应^[11]；④流体不混溶^[12~14]。其中，流体不混溶的证据主要来自含 CO₂ 的流体包裹体，这种包裹体在南岭地区锡田^[15]、盘古山^[16]、大吉山^[17]、茅坪^[18]等多个石英脉型钨矿中发现。Liu^[19]利用计算模拟发现，水力破裂后热液中 CO₂ 的溶解度可下降 36%。然而，降压后 CO₂ 逃逸如何改变热液化学平衡和钨溶解度有待定量模型的进一步评价。文章通过 NaCl-H₂O-CO₂ 体系反应平衡模型定量分析 CO₂ 逃逸对钨溶解度的影响，以探讨其是否为黑钨矿有效沉淀机制。

1 研究背景

石英脉型黑钨矿床是重要的钨矿床类型之一，主要分布于江西、湖南、广东、广西等地^[2,4,6]。含黑钨矿的石英脉近垂直分布在碱长花岗岩顶部接触带附近^[20]，延伸约 1 km^[21~23]。矿石矿物和脉石矿物的流体包裹体研究结果表明钨成矿流体是 NaCl-H₂O±CO₂ 体系，成矿温度一般在 300 ℃ ~ 400 ℃，压力可达 90 ~ 200 MPa，盐度通常不超过 10wt% NaCl，相关实验数据来自大吉山^[8,17]、瑶岗仙^[9,24,25]、锡田^[11]、盘古山^[16,26]、茅坪^[18]、淘锡坑^[27,28]、漂塘^[29,30]、黄沙^[31]、西华山^[32,33]等石英脉型钨矿床。该类型矿床的产出深度约 4 ~ 8 km^[5,32,34]。

目前已在黑钨矿、黄玉、石英等矿石和脉石矿物中发现含 CO₂ 的包裹体，相关研究表明 CO₂ 逃逸触发的流体不混溶是黑钨矿沉淀的重要机制^[18,35~36]。CO₂ 是热液中一种较为常见的挥发份^[37~39]，也是热液酸碱平衡的缓冲剂^[40]。压力降低会使热液中 CO₂ 逃逸，引起 pH 升高，从而可能造成矿物质沉淀^[13,40]。故有必要定量地评价 CO₂

逃逸对黑钨矿溶解度的影响。

2 反应平衡模型

地球化学反应平衡模型是以平衡热力学和反应动力学为理论基础，利用数值计算方法，求解相应的非线性方程组，得出研究体系中化学组分的存在形式、浓度和活性等有关信息^[41]。该方法已在斑岩型铜矿^[42~44]、不整合型铀矿^[45~46]、热液型金矿^[47]等多种类型矿床的成矿作用动力学机制研究中发挥重要作用。有学者曾利用含钨体系的反应平衡模型定量分析在钨溶解度与温度、压力、盐度和 pH 的关系，其中 Heinrich^[48] 研究了锡钨在盐水体系的溶解度模型，Gibert 等^[49] 和龚庆杰等^[50] 的平衡反应模型主要针对白钨矿，而 Wood 和 Sammon^[51] 关于黑钨矿和白钨矿的溶解度模型最为全面；然而，以往的模型都未考虑 CO₂ 在水溶液的离解反应。文章通过建立 W-Fe-Cl-Na-O-C-H 体系的反应平衡模型，定量分析 CO₂ 逃逸对钨溶解度的影响。

反应平衡模型考虑了 H⁺、OH⁻、HCl⁰、Cl⁻、Na⁺、NaCl⁰、NaOH⁰、H₂WO₄⁰、HWO₄⁻、WO₄²⁻、NaWO₄⁻、NaHWO₄⁰、Fe²⁺、FeCl⁺、FeCl₂⁰、FeOH⁺、FeO⁰、HFeO₂⁻、FeWO₄ (s)、CO₂ (aq)、HCO₃⁻ 和 CO₃²⁻ 共 22 种组分，涉及 16 个化学反应（表 1）及 4 个电荷和质量守恒方程（表 2）。FeWO₄ (s) 离解常数、NaWO₄⁻ 和 NaHWO₄⁰ 的缔合常数根据 Wood 和 Samson^[51] 提出经验公式计算，其余 13 个化学反应的平衡常数根据 SUPCRT 数据库的热力学参数计算^[52]。CO₂ 溶解度根据毛世德^[53] 提出的公式计算。有电荷组分的活度系数根据扩展 Deby-Hückel 方程计算^[54]；CO₂ 的活度系数根据 Drummond 提出的经验方程计算^[55]，其余电中性组分的活度系数为 1。上述平衡常数计算和非线性方程组求解在开源程序 R 下完成。模型所用参数分别为：温度 300 ~ 400 ℃，压力 40 ~ 200 MPa，盐度 10wt% NaCl，静水压力梯度 10 MPa/km，静岩压力梯度 25 MPa/km，深度 4 ~ 8 km。利用 R 语言程序包 CHNOSZ 计算表 1 中的反应平衡常数和有电荷组分的活度系数。FeWO₄ (s) 和 CO₂ (aq) 不必求解，故有 20 个变量，上述 20 个非线性方程求解利用 R 语言程序包 rootSolve 完成。

表 1 平衡反应模型中的 16 个化学反应

Table 1 The 16 reactions used in the thermodynamic model of this study

序号	化学反应
1	$\text{H}^+ + \text{WO}_4^{2-} = \text{HWO}_4^-$
2	$\text{H}^+ + \text{HWO}_4^- = \text{H}_2\text{WO}_4^0$
3	$\text{H}^+ + \text{Cl}^- = \text{HCl}^0$
4	$\text{H}_2\text{O} = \text{H}^+ + \text{OH}^-$
5	$\text{FeWO}_4 (\text{s}) = \text{Fe}^{2+} + \text{WO}_4^{2-}$
6	$\text{Fe}^{2+} + \text{Cl}^- = \text{FeCl}^+$
7	$\text{Fe}^{2+} + 2\text{Cl}^- = \text{FeCl}_2^0$
8	$\text{Fe}^{2+} + \text{H}_2\text{O} = \text{FeOH}^+ + \text{H}^+$
9	$\text{Fe}^{2+} + \text{H}_2\text{O} = \text{FeO}^0 + 2\text{H}^+$
10	$\text{Fe}^{2+} + 2\text{H}_2\text{O} = \text{HFeO}_2^- + 3\text{H}^+$
11	$\text{Na}^+ + \text{Cl}^- = \text{NaCl}^0$
12	$\text{Na}^+ + \text{H}_2\text{O} = \text{NaOH}^+ + \text{H}^+$
13	$\text{Na}^+ + \text{WO}_4^{2-} = \text{NaWO}_4^-$
14	$\text{Na}^+ + \text{HWO}_4^- = \text{NaHWO}_4^0$
15	$\text{CO}_2 (\text{aq}) + \text{H}_2\text{O} = \text{HCO}_3^- + \text{H}^+$
16	$\text{HCO}_3^- = \text{CO}_3^{2-} + \text{H}^+$

3 计算结果

平衡反应模型计算结果如下:

(1) 在热液温度达到 300 °C 时, CO_2 溶解度可达到 2~10 mol/kg H_2O (图 1a); CO_2 溶解度与压力成正相关关系; 当流体压力从静岩压力降至静水压力水平, CO_2 溶解度下降 55%~57%。相比 300 °C 的溶解度线, 400 °C 热液的 CO_2 溶解度显著提高, 最高可达到 25 mol/kg H_2O (图 1b); 当流体压力从静岩压力降至静水压力水平, CO_2 溶解度下降 74%~82%。

(2) pH 与压力呈负相关关系 (图 2)。300 °C 的热液 pH 为 3.08~3.91; 当流体压力从静岩压力降至静水压力水平, 热液 pH 上升 0.4~0.5。400 °C 的热液 pH 范围是 3.58~5.42; 当流体压力从静岩

表 2 平衡反应模型中所用的电荷和质量平衡方程

Table 2 Mass and charge balance constraints used in the thermodynamic model

序号	名称	电荷和质量平衡方程
17	电荷平衡方程	$[\text{H}^+] + [\text{Na}^+] + [\text{FeCl}^+] + 2[\text{Fe}^{2+}] + [\text{FeOH}^+] = [\text{HWO}_4^-] + 2[\text{WO}_4^{2-}] + [\text{Cl}^-] + [\text{OH}^-] + [\text{HFeO}_2^-] + [\text{HCO}_3^-] + 2[\text{CO}_3^{2-}]$
18	氯质量平衡方程	$\Sigma \text{Cl} = [\text{Cl}^-] + [\text{HCl}^0] + [\text{NaCl}^0] + [\text{FeCl}^+] + 2[\text{FeCl}_2^0]$
19	$\Sigma \text{Fe} = \Sigma \text{W}$	$[\text{H}_2\text{WO}_4^0] + [\text{HWO}_4^-] + [\text{WO}_4^{2-}] = [\text{FeCl}^+] + [\text{FeCl}_2^0] + [\text{Fe}^{2+}] + [\text{FeOH}^+] + [\text{FeO}^0] + [\text{HFeO}_2^-]$
20	CO_2 含量固定	在给定的温度、压力和盐度条件下, CO_2 含量达到溶解度 (根据文献 [53] 公式计算)

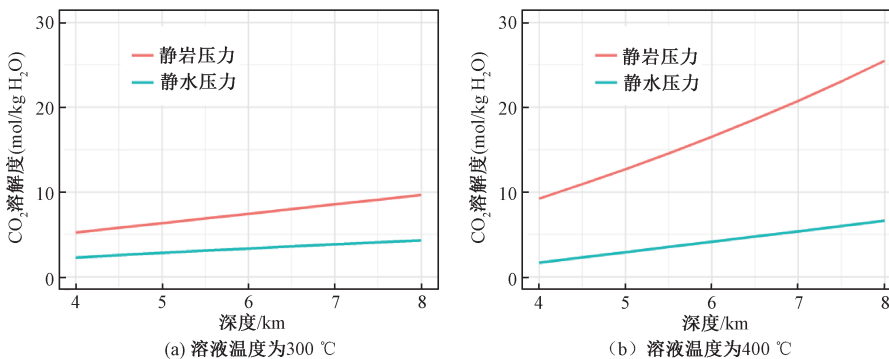
图 1 在 4~8 km 深度的静岩压力和静水压力下 CO_2 溶解度等温变化曲线

Fig. 1 The isothermal change of CO_2 solubility under the lithostatic and hydrostatic levels at a depth of 4~8 km

压力降至静水压力水平, 热液 pH 上升 0.9~1.2。

(3) 钨溶解度与压力呈正相关关系 (图 3)。当热液温度达到 300 °C, 钨溶解度 8.19×10^{-6} ~ 18.05×10^{-6} ; 压力从静岩压力降至静水压力水平后, 钨溶解度下降 3.08×10^{-6} ~ 7.88×10^{-6} , 降幅 27.3%~43.7%, 平均降幅 36.0%。400 °C 的热液钨溶解度 59.97×10^{-6} ~ 155.41×10^{-6} ; 流体压力从

静岩压力降至静水压力水平后, 钨溶解度下降 33.80×10^{-6} ~ 72.50×10^{-6} , 降幅 36%~47%, 平均降幅 41%。降幅比例与深度成正比。

(4) 由图 4 可知, 含钨组分以 HWO_4^- 为主, 其次为 NaWO_4^- 、 NaHWO_4^0 、 H_2WO_4^0 和 WO_4^{2-} 。压力从静岩压力降至静水压力水平后, HWO_4^- 的浓度显著下降。

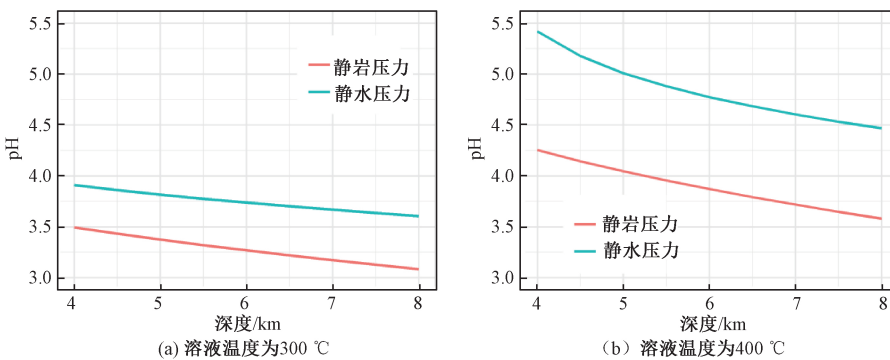


图 2 在 4~8 km 深度的静岩压力和静水压力下 pH 等温变化曲线

Fig. 2 The isothermal change of pH under the lithostatic and hydrostatic levels at a depth of 4~8 km

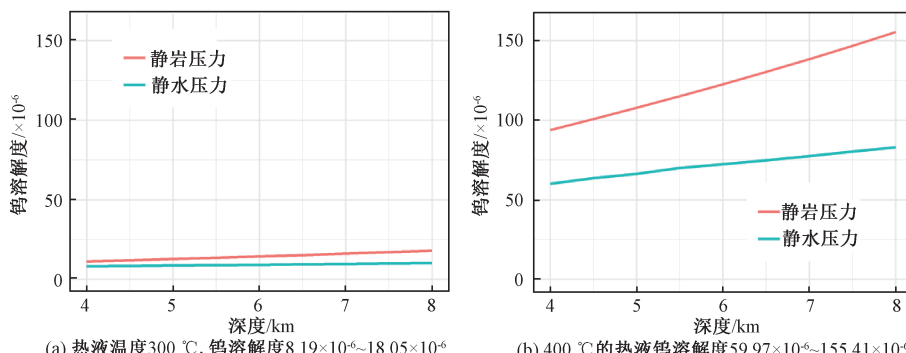


图 3 在 4~8 km 深度的静岩压力和静水压力下钨溶解度等温变化曲线

Fig. 3 The isothermal change of tungsten solubility under the lithostatic and hydrostatic levels at a depth of 4~8 km

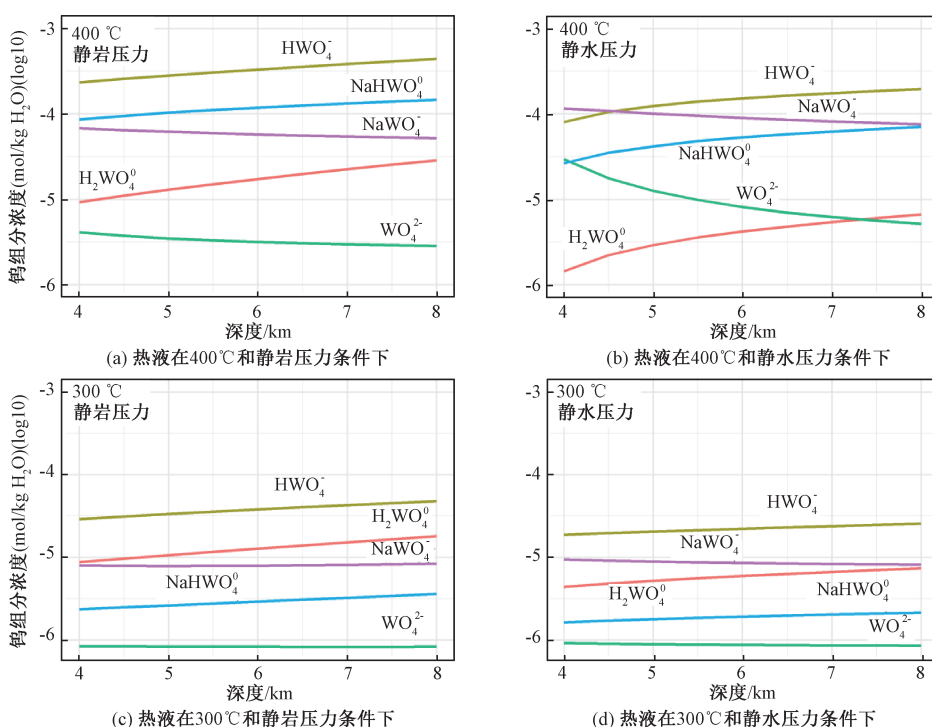


图 4 在 4~8 km 深度的静岩压力和静水压力下含钨组分等温变化曲线

Fig. 4 The isothermal change of tungsten species under the lithostatic and hydrostatic levels at a depth of 4~8 km

4 讨论与结论

目前估算南岭石英脉型黑钨矿成矿流体 pH 的研究极少, 少量国外报道的 pH 约为 4~6^[51]。这与模型中 400 °C 的热液 pH 范围接近, 但高于 300 °C 的热液 pH。已发表的数据表明大吉山钨矿和盘古山钨矿成矿流体的 CO₂ 含量已接近饱和状态^[16~17], 因而模型计算的 pH 可作为实际值的下限值; 相应地, 模型中钨溶解度降幅可作为实际值的上限值。

模型所得出的 pH 范围处于弱酸性环境。在这种环境下, Wood 和 Sammon 得出的含钨组分以 HWO₄⁻ 和 NaWO₄⁻ 为主^[51]。这与模型计算结果一致。

反应平衡模型计算结果表明, 在 4~8 km 的成矿深度下, 降压造成的 CO₂ 逃逸可使钨溶解度下降 27%~47%; 成矿流体温度越高, 成矿深度越大, 钨溶解度降幅比例越大。位于葡萄牙的 Panasqueira 矿床是世界上最大的锡钨脉型矿床之一, 该矿床钨沉淀的效率只有 33%, 剩余 67% 被分散在矿体周边钨品位较低的围岩中^[56]。对比可知, 单纯的降压可显著降低钨在富含 CO₂ 热液中的溶解度, 因而是黑钨矿沉淀的有效机制。

致谢: 文章模型计算使用了毛世德教授提供的 CO₂ 溶解度计算程序和两个开源 R 语言程序包: Jeffrey Dick 开发的 CHNOSZ 和 Soetaert 开发的 rootSolve, 在此一并表示感谢。

参考文献/References

- [1] Mao J W, Cheng Y B, Chen M H, et al. Major types and time-space distribution of Mesozoic ore deposits in South China and their geodynamic settings [J]. Mineralium Deposita, 2013, 48 (3): 267~294.
- [2] 陈毓川, 裴荣富, 张宏良, 等. 南岭地区与中生代花岗岩类有关的有色及稀有金属矿床地质 [M]. 北京: 地质出版社, 1989.
- CHEN Yuchuan, PEI Rongfu, ZHANG Hongliang, et al. The geology of nonferrous and rare metal deposits related to Mesozoic Granitoids in Nanling Region, China [M]. Beijing: Geological Publishing Housing, 1989. (in Chinese)
- [3] 柳志青. 脉状钨矿床成矿预测理论 [M]. 北京: 科学出版社, 1980.
- LIU Zhiqing. Metallogenetic prognosis of vein-type tungsten deposits [M]. Beijing: Science Press, 1980. (in Chinese)
- [4] 朱焱龄, 李崇佑, 林运淮. 赣南钨矿地质 [M]. 南昌: 江西人民出版社, 1981.
- ZHU Yanling, LI Chongyou, LIN Yunhuai. Tungsten deposit geology in South Jiangxi Province [M]. Nanchang: Jiangxi People's Publishing House, 1981. (in Chinese)
- [5] 刘向冲. 江西大吉山石英脉型黑钨矿床“五层楼”垂直形态分带动力学机制 [D]. 北京: 中国地质大学(北京), 2014.
- LIU Xiangchong. The mechanisms of the five-floor vertical morphological zonation at the Dajishan vein-type tungsten deposit, Jiangxi [D]. Beijing: China University of Geosciences (Beijing), 2014. (in Chinese)
- [6] 祝新友, 王京彬, 王艳丽, 等. 论石英脉型钨矿成矿系统的相对封闭性——以湖南瑶岗仙脉型钨矿床为例 [J]. 地质学报, 2014, 88 (5): 825~835.
- ZHU Xinyou, WANG Jingbin, WANG Yanli, et al. Relative closed ore-forming system in the tungsten-bearing quartz vein: a case study of the Yaogangxian deposit, Hunan Province [J]. Acta Geologica Sinica, 2014, 88 (5): 825~835. (in Chinese with English abstract)
- [7] 张德会. 岩浆—热液过渡性流体及其成矿效应 [A]. 中国矿物岩石地球化学学会学术年会 [C]. 宁波, 2003.
- ZHANG Dehai. Magmatic-hydrothermal transitional fluids and its mineralization effect [A]. The Annual conference of Chinese Society for Minerology, Petrology, and Geochemistry [C]. Ningbo, 2003. (in Chinese)
- [8] Ni P, Wang X D, Wang G G, et al. An infrared microthermometric study of fluid inclusions in coexisting quartz and wolframite from Late Mesozoic tungsten deposits in the Gannan metallogenic belt, South China [J]. Ore Geology Reviews, 2015, 65: 1062~1077.
- [9] 曹晓峰, 吕新彪, 何谋春, 等. 共生黑钨矿与石英中流体包裹体红外显微对比研究——以瑶岗仙石英脉型钨矿床为例 [J]. 矿床地质, 2009, 28 (5): 611~620.
- CAO Xiaofeng, LV Xinbiao, HE Mouchun, et al. An infrared microscope investigation of fluid inclusions in coexisting quartz and wolframite: A case study of Yaogangxian quartz-vein wolframite deposit [J]. Mineral Deposits, 2009, 28 (5): 611~620. (in Chinese with English abstract)
- [10] Wei W F, Hu R Z, Bi X W, et al. Infrared microthermometric and stable isotopic study of fluid inclusions in wolframite at the Xihuashan tungsten deposit, Jiangxi province, China [J]. Mineralium Deposita, 2012, 47 (6): 589~605.
- [11] Lecumberri-Sanchez P, Vieira R, Heinrich C A, et al. Fluid-rock interaction is decisive for the formation of tungsten deposits [J]. Geology, 2017, 45 (7): 579~582.
- [12] Polya D A. Pressure-Independence of Wolframite solubility for Hydrothermal Vein Formation [J]. Transactions of the Institution of Mining and Metallurgy, 1990, 99 (B59): 120~124.
- [13] Korges M, Weis P, Lüders V, et al. Depressurization and boiling of a single magmatic fluid as a mechanism for tin-tungsten deposit formation [J]. Geology, 2017, 46 (1): 75~78.

- [14] 张生, 陈根文. 钨的气态迁移与岩浆-热液成矿作用: 实验研究及其成矿学意义 [J]. 地质科学, 2015, 50 (3): 898~910.
- ZHANG Sheng, CHEN Genwen. Gaseous transport and magmatic-hydrothermal mineralization of tungsten: experimental study and its metallogenetic implications [J]. Chinese Journal of Geology, 2015, 50 (3): 898~910. (in Chinese with English abstract)
- [15] Xiong Y Q, Shao Y J, Zhou H D, et al. Ore-forming mechanism of quartz-vein-type W-Sn deposits of the Xitian district in SE China: Implications from the trace element analysis of wolframite and investigation of fluid inclusions [J]. Ore Geology Reviews, 2017, 83: 152~173.
- 王旭东, 倪培, 张伯声, 等. 江西盘古山石英脉型钨矿床流体包裹体研究 [J]. 岩石矿物学杂志, 2010, 29 (5): 539~550.
- WANG Xudong, NI Pei, ZHANG Bosheng, et al. Fluid inclusion studies of the Pangushan quartz-vein type tungsten deposit in southern Jiangxi Province [J]. Acta Petrologica Et Mineralogica, 2010, 29 (5): 539~550. (in Chinese with English abstract)
- [16] 席斌斌, 张德会, 周利敏, 等. 江西省全南县大吉山钨矿成矿流体演化特征 [J]. 地质学报, 2008, 82 (7): 956~966.
- XI Binbin, ZHANG Dehai, ZHOU Limin, et al. Characteristics of ore-forming fluid evolution in Dajishan tungsten deposit, Quannan County, Jiangxi [J]. Acta Geologica Sinica, 2008, 82 (7): 956~966. (in Chinese with English abstract)
- [17] 周龙全, 李光来, 苏晔, 等. 赣南茅坪钨矿床黄玉单晶流体包裹体研究 [J]. 矿床地质, 2017, 36 (4): 921~934.
- ZHOU Longquan, LI Guanglai, SU Ye, et al. A preliminary study of fluid inclusions of topaz crystal from Maoping tungsten deposit, southern Jiangxi Province [J]. Mineral Deposits, 2017, 36 (4): 921~934. (in Chinese with English abstract)
- [18] Liu X C, Xing H L, Zhang D H. Influences of hydraulic fracturing on fluid flow and mineralization at the vein-type tungsten deposits in southern China [J]. Geofluids, 2017, 2017: Article ID 4673421.
- [19] 祝新友, 王京彬, 王艳丽, 等. 南岭锡钨多金属矿区碱长花岗岩的厘定及其意义 [J]. 中国地质, 2012, 39 (2): 359~381.
- ZHU Xinyou, WANG Jingbin, WANG Yanli, et al. Characteristics of alkali feldspar granite in tungsten (tin) deposits of Nanling region [J]. Geology in China, 2012, 39 (2): 359~381. (in Chinese with English abstract)
- [20] 古菊云. 华南钨矿脉的形态分类 [A]. 钨矿地质讨论会论文集 [C]. 北京: 地质出版社, 1984, 35~45.
- Gu Juyun. Morphological zonation of tungsten deposits in South China [A]. Proceedings of Symposium on Tungsten Geology [C]. Beijing: Geological Publishing House, 1984, 35~45. (in Chinese)
- [21] 刘向冲, 张德会, 赵波, 等. 漂塘钨矿床“五层楼”垂直形态分带定量分析 [J]. 高校地质学报, 2017, 23 (3): 408~416.
- LIU Xiangchong, ZHANG Dehai, ZHAO Bo, et al. Quantitative analysis of the “five-floor” vertical morphological zonation in the Piaotang tungsten deposits, South China [J]. Geological Journal of China Universities, 2017, 23 (3): 408~416. (in Chinese with English abstract)
- [22] 李吉明, 李永明, 楼法生, 等. 赣北发现“五层楼”式石英脉型黑钨矿矿床——东坪黑钨矿矿床的发现及其地质意义 [J]. 地球学报, 2016, 37 (3): 379~384.
- LI Jiming, LI Yongming, LOU Fasheng, et al. A “five-storey” style quartz vein wolframite deposit in northern Jiangxi province: the discovery of the dongping wolframite deposit and its geological significance [J]. Acta Geoscientica Sinica, 2016, 37 (3): 379~384. (in Chinese with English abstract)
- [23] 李少花, 毕献武, 胡瑞忠, 等. 湖南瑶岗仙石英脉型黑钨矿床成矿流体特征 [J]. 矿物岩石, 2011, 31 (2): 54~60.
- DONG Shaohua, BI Xianwu, HU Ruizhong, et al. Characteristics of ore-forming fluid in Yaogangxian quartz-vein wolframite deposit, Hunan Province [J]. Journal of Mineralogy and Petrology, 2011, 31 (2): 54~60. (in Chinese with English abstract)
- [24] 王巧云, 胡瑞忠, 彭建堂, 等. 湖南瑶岗仙钨矿床流体包裹体特征及其意义 [J]. 岩石学报, 2007, 23 (9): 2263~2273.
- WANG Qiaoyun, HU Ruizhong, PENG Jiantang, et al. Characteristics and significance of the fluid inclusions from Yaogangxian tungsten deposit in south of Hunan [J]. Acta Petrologica Sinica, 2007, 23 (9): 2263~2273. (in Chinese with English abstract)
- [25] 叶诗文, 路远发, 童启荃, 等. 盘古山钨矿成矿流体特征及其地质意义 [J]. 华南地质与矿产, 2014, 30 (1): 26~35.
- YE Shiwen, LU Yuanfa, TONG Qiquan, et al. Fluid inclusion characteristic and its geological implication of the Pangushan tungsten deposit [J]. Geology and Mineral Resources of South China, 2014, 30 (1): 26~35. (in Chinese with English abstract)
- [26] 宋生琼, 胡瑞忠, 毕献武, 等. 赣南海锡坑钨矿床流体包裹体地球化学研究 [J]. 地球化学, 2011, 40 (3): 237~248.
- SONG Shengqiong, HU Ruizhong, BI Xianwu, et al. Fluid inclusion geochemistry of the Taoxikeng tungsten deposit in southern Jiangxi Province, China [J]. Geochimica, 2011, 40 (3): 237~248. (in Chinese with English abstract)
- [27] 宋生琼, 胡瑞忠, 毕献武, 等. 赣南崇义淘锡坑钨矿床氢、氧、硫同位素地球化学研究 [J]. 矿床地质, 2011, 30 (1): 1~10.
- SONG Shengqiong, HU Ruizhong, BI Xianwu, et al. Hydrogen, oxygen and sulfur isotope geochemical characteristics of Taoxikeng tungsten deposit in Chongyi County, Southern Jiangxi Province [J]. Mineral Deposits, 2011, 30 (1): 1~10. (in Chinese with English abstract)
- [28] 王旭东, 倪培, 蒋少涌, 等. 赣南漂塘钨矿床流体包裹体研究 [J]. 岩石学报, 2008, 24 (9): 2163~2170.

- [30] 王旭东, 倪培, 袁顺达, 等. 赣南漂塘钨锡石及共生石英中流体包裹体研究 [J]. 地质学报, 2013, 87 (6): 850~859.
- WANG Xudong, NI Pei, YUAN Shunda, et al. Fluid inclusion studies on coexisting cassiterite and quartz from the Piaotang tungsten deposit, Jiangxi Province, China [J]. Acta Petrologica Sinica, 2008, 24 (9): 2163~2170. (in Chinese with English abstract)
- [31] 王旭东, 倪培, 袁顺达, 等. 江西黄沙石英脉型钨矿床流体包裹体研究 [J]. 岩石学报, 2012, 28 (1): 122~132.
- WANG Xudong, NI Pei, YUAN Shunda, et al. Fluid inclusion studies of the Huangsha quartz-vein type tungsten deposit, Jiangxi Province [J]. Acta Petrologica Sinica, 2012, 28 (1): 122~132. (in Chinese with English abstract)
- [32] 黄惠兰, 常海亮, 付建明, 等. 西华山脉钨矿床的形成压力及有关花岗岩的侵位深度 [J]. 矿床地质, 2006, 25 (5): 562~571.
- HUANG Huilan, CHANG Hailiang, FU Jianming, et al. Formation pressure of wolframite-vein deposits and emplacement depth of related granite in Xihuashan, Jiangxi Province [J]. Mineral Deposits, 2006, 25 (5): 562~571. (in Chinese with English abstract)
- [33] 王碟, 卢焕章, 毕献武. 与花岗质岩浆系统有关的石英脉型钨矿和斑岩型铜矿成矿流体特征比较 [J]. 地学前缘, 2011, 18 (5): 121~131.
- WANG Die, LU Huanzhang, BI Xianwu. Comparison of characteristics of ore forming fluids between quartz-vein tungsten deposits and porphyry copper deposits associated with granitic rocks [J]. Earth Science Frontiers, 2011, 18 (5): 121~131. (in Chinese with English abstract)
- [34] 范宗瑶, 李荫清, 王龙生, 等. 从流体包裹体研究探讨金属矿床成矿条件 [J]. 矿床地质, 2003, 22 (1): 13~23.
- RUI Zongyao, LI Yingqing, WANG Longsheng, et al. Approach to ore-forming conditions in light of ore fluid inclusions [J]. Mineral Deposits, 2003, 22 (1): 13~23. (in Chinese with English abstract)
- [35] Chen L L, Ni P, Li W S, et al. The link between fluid evolution and vertical zonation at the Maoping tungsten deposit, Southern Jiangxi, China: Fluid inclusion and stable isotope evidence [J]. Journal of Geochemical Exploration, 2018, 192: 18~32.
- Li W S, Ni P, Pan J Y, et al. Fluid inclusion characteristics as an indicator for tungsten mineralization in the Mesozoic Yaogangxian tungsten deposit, central Nanling district, South China [J]. Journal of Geochemical Exploration, 2018, 192: 1~17.
- [36] 范宏瑞, 胡芳芳, 杨进辉, 等. 胶东中生代构造体制转折过程中流体演化和金的大规模成矿 [J]. 岩石学报, 2005, 21 (5): 1317~1328.
- FAN Hongrui, HU Fangfang, YANG Jinhui, et al. Fluid evolution and large-scale gold metallogeny during Mesozoic tectonic transition in the eastern Shandong province [J]. Acta Petrologica Sinica, 21 (5): 1317~1328. (in Chinese with English abstract)
- [38] 倪培, 迟哲, 潘君屹, 等. 热液矿床的成矿流体与成矿机制——以中国若干典型矿床为例 [J]. 矿物岩石地球化学通报, 2018, 37 (3): 369~395.
- NI Pei, CHI Zhe, PAN Junyi, et al. The characteristics of ore-forming fluids and mineralization mechanism in hydrothermal deposits: a case study of some typical deposits in China [J]. Bulletin of Mineralogy, Petrology and Geochemistry, 2018, 37 (3): 369~395. (in Chinese with English abstract)
- [39] 徐九华, 张国瑞, 魏浩, 等. 脉状金矿床的成矿压力与深度: 流体包裹体方法及其影响因素 [J]. 南京大学学报(自然科学), 2012, 48 (3): 266~277.
- XU Jiuhua, ZHANG Guorui, WEI Hao, et al. Ore-forming pressures and depths of vein gold deposits: fluid inclusion studies and their influence factors [J]. Journal of Nanjing University (Natural Sciences), 2012, 48 (3): 266~277. (in Chinese with English abstract)
- [40] 冷成彪, 张兴春, 王守旭, 等. 岩浆—热液体系成矿流体演化及其金属元素气相迁移研究进展 [J]. 地质论评, 2009, 55 (1): 100~112.
- LENG Chengbiao, ZHANG Xingchun, WANG Shouxu, et al. Advances of researches on the evolution of ore-forming fluids and the vapor transport of metals in magmatic-hydrothermal systems [J]. Geological Review, 2009, 55 (1): 100~112. (in Chinese with English abstract)
- [41] 陈家玮, 鲍征宇. 地球化学反应平衡模型的建模方法 [J]. 地质科技情报, 2001, 20 (3): 41~46.
- CHEM Jiawei, BAO Zhengyu. Approaches to geochemical reaction equilibrium modeling [J]. Geological Science and Technology Information, 2001, 20 (3): 41~46. (in Chinese with English abstract)
- [42] 周涛发, 刘晓东, 袁峰, 等. 安徽月山矿田成矿流体中铜、金的迁移形式和沉淀的物理化学条件 [J]. 岩石学报, 2000, 16 (4): 551~558.
- ZHOU Taofa, LIU Xiaodong, YUAN Feng, et al. Migrating forms and depositional physicochemical conditions of copper, gold in hydrothermal solutions of Yueshan orefield, Anhui province [J]. Acta Petrologica Sinica, 2000, 16 (4): 551~558. (in Chinese with English abstract)
- [43] 周涛发, 袁峰, 岳书仓, 等. 安徽月山矿田夕卡岩型矿床形成的水岩作用 [J]. 矿床地质, 2002, 21 (1): 1~9.
- ZHOU Taofa, YUAN Feng, YUE Shucang, et al. Water/rock interaction during formation of skarn-type deposits in Yueshan Orefield, Anhui Province [J]. Mineral Deposits, 2002, 21 (1): 1~9. (in Chinese with English abstract)
- [44] Heinrich C A. The physical and chemical evolution of low-salinity magmatic fluids at the porphyry to epithermal transition:

- a thermodynamic study [J]. *Mineralium Deposita*, 2005, 39 (8): 864~889.
- [45] Aghbelagh Y B, Yang J W. Effect of graphite zone in the formation of unconformity-related uranium deposits: Insights from reactive mass transport modeling [J]. *Journal of Geochemical Exploration*, 2014, 144: 12~27.
- [46] Aghbelagh Y B, Yang J W. Role of hydrodynamic factors in controlling the formation and location of unconformity-related uranium deposits: insights from reactive-flow modeling [J]. *Hydrogeology Journal*, 2017, 25 (2): 465~486.
- [47] Hofstra A H, Leventhal J S, Northrop H R, et al. Genesis of sediment-hosted disseminated-gold deposits by fluid mixing and sulfidization: Chemical-reaction-path modeling of ore-depositional processes documented in the Jerritt Canyon district, Nevada [J]. *Geology*, 1991, 19 (1): 36~40.
- [48] Heinrich C A. The chemistry of hydrothermal tin (-tungsten) ore deposition [J]. *Economic Geology*, 1990, 85 (3): 457~481.
- [49] Gibert F, Moine B, Schott J, et al. Modeling of the transport and deposition of tungsten in the scheelite-bearing calc-silicate gneisses of the Montagne Noire, France [J]. *Contributions to Mineralogy and Petrology*, 1992, 112 (2~3): 371~384.
- [50] 龚庆杰, 于崇文, 张荣华. 柿竹园钨多金属矿床形成机制的物理化学分析 [J]. 地学前缘, 2004, 11 (4): 617~625.
GONG Qingjie, YU Chongwen, ZHANG Ronghua. Physical chemistry study on the ore-forming process of Shizhuyuan tungsten-polymetallic deposit [J]. *Earth Science Frontiers*, 2004, 11 (4): 617~625. (in Chinese with English abstract)
- [51] Wood S A, Samson I M. The hydrothermal geochemistry of Tungsten in Granitoid environments: I. Relative solubilities of ferberite and scheelite as a function of T, P, pH, and m_{NaCl} [J]. *Economic Geology*, 2000, 95 (1): 143~182.
- [52] Johnson J W, Oelkers E H, Helgeson H C. SUPCRT92: A software package for calculating the standard molal thermodynamic properties of minerals, gases, aqueous species, and reactions from 1 to 5000 bar and 0 to 1000°C [J]. *Computers & Geosciences*, 1992, 18 (7): 899~947.
- [53] Mao S D, Zhang D H, Li Y Q, et al. An improved model for calculating CO_2 solubility in aqueous NaCl solutions and the application to $\text{CO}_2\text{-H}_2\text{O-NaCl}$ fluid inclusions [J]. *Chemical Geology*, 2013, 347: 43~58.
- [54] Helgeson H C. Thermodynamics of hydrothermal systems at elevated temperatures and pressures [J]. *American Journal of Science*, 1969, 267 (7): 729~804.
- [55] Drummond S E Jr. Boiling and mixing of hydrothermal fluids: chemical effects on mineral precipitation [D]. Pennsylvania: Pennsylvania State University, 1981.
- [56] Polya D A. Efficiency of hydrothermal ore formation and the Panasqueira W-Cu (Ag)-Sn vein deposit [J]. *Nature*, 1988, 333 (6176): 838~841.